Royal Norwegian Council
for Scientific and Industrial Research
(NTNF)

NORSAR

NORSAR Scientific Report No. 2-89/90

Semiannual Technical Summary

1October 1989 — 31 March 1990

Kjeller, June 1990

APPROVED FOR PUBLIC RELEASE, DISTRIBUTION UNLIMITED

7.6 Application of the threshold monitoring method

The concept of threshold monitoring was introduced by Ringdal and Kværna (1989) as a method of monitoring the seismic amplitude levels for the purpose of using this information to assess the largest size of events that might go undetected. In an effort to demonstrate the capabilities of this threshold monitoring concept, a preliminary version has been implemented into the Intelligent Monitoring System (IMS) (Bache *et al*, 1990). A demonstration of this implementation was given at the Symposium on Regional Seismic Arrays and Nuclear Test Ban Verification, held in Oslo in February 1990. In the following, we will present figures from that demonstration, as well as a brief description of the method.

Method description

The basic idea behind the threshold monitor is, for any given point in time, to infer the upper magnitude limit of a possible seismic event at a given geographical location. By combining observations of the amplitude of the seismic data at different arrays and/or single stations, we can apply the formalism developed by Ringdal and Kværna (1989) to compute an upper magnitude limit based on the network.

In order to apply this method the following procedure is required:

- For each location-station-phase combination, estimate continuously the seismic amplitude levels. If the station is an array, we use STA values of filtered beams to represent the amplitude levels. The steering parameters of the beams will then correspond to the apparent velocity and azimuth of the actual phase. The filter bands are chosen such that good SNR is ensured. If the observation unit is a single station, the STA values are computed from a filtered channel.

- When considering a potential event at a given time and location, measure the seismic amplitude levels at the expected arrival times for the relevant seismic phases. The travel times for each phase can be taken from standard travel time tables, or by processing events with known location and origin time.

- In order to relate the STA observations to actual magnitude estimates, apply the formula

$$m = log(STA) + b$$

  where b is a correction factor for each location-station-phase combination. The correction factors can be obtained by processing events with known magnitudes, or by using standard attenuation values.

- For assessing the significance of our magnitude estimates, assume that they are sampled from a normal distribution with a given standard deviation. Based on experience with signal amplitude variation across the NORSAR array, we have used a preliminary value of 0.2 for a small epicentral area.

- The magnitude limits computed by this algorithm are tied to a given confidence level, here set to 0.9. This means that the estimated limits represent the largest magnitude of a possible hidden event, in the sense that there is at least a 90 per cent probability that one or more of the observed amplitude values would be exceeded by the signals from an event with magnitude above these limits.

Interfering events

To illustrate the capability of the threshold monitor in the presence of an interfering event, we assume a situation as shown in Fig. 7.6.1. A teleseismic event is interfering with a local mining explosion, causing large amplitudes at the expected arrival time of Pn. We also assume that we are monitoring the source region of the actual mining explosion, using appropriate calibration values for the seismic phases considered.

If we now compute an upper magnitude limit only from the amplitude level at the time of the Pn arrival (where the interfering event is added), we will necessarily conclude that a relatively large explosion may have occurred. If we in addition bound the event magnitude by the undisturbed Lg amplitude, we will get a much lower value.

An actual interfering event situation may in fact be more complex than this, e.g. one station may be contaminated with high amplitudes for a long time period, or may even not record data. In such cases, amplitudes recorded at other stations may put strong constraints on the upper magnitude limit, and thereby exclude the possible occurence of a strong event.

Beamforming

The beamforming capability of regional arrays is efficiently exploited by the threshold monitor, both for P and S-phases. The STA traces used in the computation of the upper magnitude limits are derived from the amplitudes of filtered steered beams. At NORESS, we know that forming Pn beams will reduce the amplitude level of pure noise by about 14 dB (Kværna, 1989). For optimally steered Pn beams, the signal loss will be less than 3 dB for frequencies below 6 Hz. This will cause the calibration factors (b-values) to increase with the same amount, but we will still lower the upper magnitude limit by more than 10 dB (0.5 magnitude units).

For Lg, we expect the noise suppression to be somewhat less than for Pn, and we also expect a higher signal loss. Nevertheless, a reduction of the upper magnitude limit by more than 6 dB seems to be feasible for Lg.

Signals arriving from events outside the monitoring region may have their amplitudes significantly reduced by beamforming. The amount of amplitude reduction depend on the difference between the slowness vectors of the beam and the arriving signal, as well as on the beampattern of the array.

Implementation

In the present demonstration we use data from the three regional arrays in Fennoscandia: NORESS, ARCESS and FINESA. As target regions for threshold monitoring, we have chosen 10 active mining regions in Fennoscandia and Western USSR, as well as the Soviet nuclear test site at Shagan River (see Table 7.6.1).

For the 10 mining regions, the phases Pn and Lg at each array are being used to infer the upper magnitude limits. Calibration factors are found by processing events with magnitudes reported in the regional seismic bulletin of the University of Helsinki. Travel times and beamsteering parameters are obtained from the same processing. The filter bands for Pn and Lg are respectively 3–5 Hz and 1.5–3.5 Hz, and the STA sampling interval is set to 1 second. For Pn, the STA integration window is 2 seconds, and maximum STA is chosen within ± 2 seconds of the predicted arrival time. The reason why the amplitude level is represented by the maximum STA within a certain time tolerance, is that each target point represents a finite region, e.g. 10x10 km, and that phases from events occuring outside the center point will have somewhat different travel times. The STA integration window for Lg is 10 seconds, with maximum chosen within ± 3 seconds of the predicted arrival time. For distances less than 500 km, however, the integration window for Lg is reduced to 5 seconds.

For the Shagan River test site, calibration factors, travel times and beamsteering parameters for the phases P, PP and PcP were obtained from processing events with known magnitude and location. This was done for both ARCESS and NORESS, but as no observations were available for the FINESA array, the calibration factors were temporarily set to the same values as those of the ARCESS array. Travel times and apparent velocities are taken from standard tables, and the receiver-source azimuth is used. The STA integration windows are 2 seconds for P, and 5 seconds for PP and PcP. Time tolerances are 2 seconds for P and 3 seconds for PP and PcP.

The data processing flow can be outlined as follows:

- Compute filtered beams and STA traces for each array. The STA traces are stored on cyclic files, containing the last 5 days of data.
- Compute upper magnitude limits from the network of arrays, as well as from each array separately. The program reads the STA traces from the cyclic files, and stores the resulting magnitude traces on new cyclic files, also these containing the last 5 days of data. The total size of the files is altogether about 96 Mb.
- Analyze the magnitude traces by an interactive process within the IMS. Magnitude data are read from the cyclic files and displayed as continuous time series. The interactive processing is also attached to the IMS event data base, such that information on interesting events can be retrieved, e.g. by showing the location, origin time and estimated magnitude.

Examples from the demonstration

Fig. 7.6.2 shows the location of the 10 mining regions used as target areas for the threshold monitoring. In the following example, we will concentrate on the mine HC17. In addition to the upper magnitude limits derived from the network of arrays, upper magnitude limits were computed from each array separately. Fig. 7.6.3 shows these traces for Friday 02/03/90. The first 6 hours of the day are charcterized by low seismic noise levels, and any events at HC17 must have magnitudes well below 1.5. The low seismic activity is also illustrated by the V's on top of each curve, indicating origin times of events located by the IMS. An increase in the seismic amplitude level caused by an event shows up like spikes on the graphs. As expected, these occurrences are much more frequent during working hours (07-15 GMT). At NORESS, there is also a general increase in the background noise level during these hours. This is probabaly caused by nearby industrial activity (Fyen *et al*, 1990; Kværna, 1990).

From Fig. 7.6.2 we see that while the upper magnitude limits computed from each array separately indicate several time intervals where events with magnitudes greater that 2.0 may have occured at HC17, the network curve efficiently exclude all but two of these cases. The program allows us to expand the plots, so that interesting time intervals can be investigated. This is done in Figure 4, expanding Fig. 7.6.3 for a time interval around 12 GMT. The two interesting instances (called Event 1 and Event 2) are identified on the plot.

On Fig. 7.6.4 we see that the IMS has found events with origin times close to the peaks. By clicking on the V's with the mouse, the corresponding event location is sent to the map for display. Fig. 7.6.5 shows the map with

the locations of Event 1 and Event 2. Event 1 is in fact occuring at HC17, whereas Event 2 is located approximately 400 km further south.

These two events illustrate well some main features of the threshold monitoring technique, and we will comment upon them in some detail:

Event 1, located in the target region

In the case of Event 1, located at HC17, we note that this event was sufficiently large to have phase detections (both P and Lg) at all three arrays. The threshold monitor algorithm project the observations back to origin times at the target region, so with an event occuring at the target region, the corresponding peaks should line up for all four curves in Fig. 7.6.4. In addition, we expect the upper magnitude limits computed from each array separately, to approach the same value, provided that each array has peaks exceeding the background noise level. For Event 1, both of these features are clearly seen. In the IMS bulletin, the magnitude of the event is estimated to 1.6, whereas the Helsinki magnitude value is 2.2. This difference is attributed to different calibration factors, and it appears that the IMS in general gives lower magnitude values than Helsinki.

The network trace of Fig. 7.6.4 shows an "upper limit" value of 2.2 for Event 1. It is important to be aware that this value will be slightly underestimated (as a 90 per cent upper limit) in cases when several stations actually detect the event. The reason for this is the assumption that all observed phase magnitudes are less than or equal to the observed "noise" value. In case of phase detections acually attributed to the event, the term "less than or equal to" should be replaced by "equal to" for those phases, thus arriving at a standard maximum likelihood magnitude estimation formulation (Ringdal, 1976). In practice, this makes little difference for a network of the type we are considering, but it might become more significant for larger networks. We are currently looking into ways to correct for this bias.

Our conclusion from analyzing Event 1 is that an event actually occurring in the target region will have several readily identifiable features that can be used in visually confirming the event. The threshold monitor, when operated in conjunction with a network detector, will serve to point out such occurrences.

Event 2, located outside the target region

As seen from Fig. 7.6.4, the four peaks for Event 2 do not line up very well, indicating that the epicenter is not at the monitoring region. Note also that the upper magnitude limit inferred from the network of arrays is significantly smaller than the limits inferred from each array separately. From the map in Fig. 7.6.5, we see that the event is located well away from HC17. The

IMS bulletin report a magnitude of 2.6, while the Helsinki bulletin gives a magnitude value of 2.9. The upper magnitude limit for a hypothetical event at HC17 at the time considered is found to be between 1.9 and 2.0.

In this case, the upper limit represents a realistic 90 per cent confidence threshold for such a hypothetical event. Thus we note that the method serves to ensure that (at the given confidence level), a hypothetical event occurring at HC17 would be almost a magnitude unit smaller than the nearby interfering event.

An example of teleseismic monitoring

In an attempt to show the applicability of the threshold monitoring method to teleseismic distances, we have included the Shagan River test site as a target area (Fig. 7.6.6). The distances to the three arrays are in this case between 3400 and 4300 km. We know that the NORESS array has favorable signal focusing effects for P-phases from Shagan River, and that this will make NORESS the most valuable station for constraining the magnitudes. This is clearly illustrated in Fig. 7.6.7. The network upper magnitude limits are consistently below 3.5 for 02/02/90, and are only above 3.0 when interfering seismic signals are observed at NORESS.

We note that we do not have reliable magnitude calibration functions for FINESA at the present time, and the plots in Fig. 7.6.7 should therefore be interpreted with some caution.

Conclusions and future perspectives

The implementation of the threshold monitoring method in the IMS system has shown that the method can be used in real-time operation. The displays provided by the threshold monitor appear to be very valuable in pointing out time intervals of particular interest, thus aiding the analyst in his work. The interesting intervals can be examined by different processing techniques to locate and identify the events. Our examples have demonstrated that the method can be applied both at regional and teleseismic distances. We note however, that some additional research needs to be done to assess the potential bias in the upper magnitude limits when detected phases occur from events in the target region.

A natural extension of the implementation would be to include more arrays or single stations in the processing. This can be done in a straightforward manner, as the computing algorithm is fully parametrized. Larger geographical areas can be monitored if standard amplitude-distance relationships are used to derive the magnitudes. This will require careful positioning of the target points and some research on the tuning of the processing parameters.

Acknowlegements

This research was done while one of the authors (TK) was a visiting scientist at SAIC in San Diego. Jeff Given made an extensive contribution to this project through his cooperation and knowledge of the IMS.

T. Kværna
F. Ringdal

References

Bache, T.C., S.R. Bratt, J. Wang, R.M. Fung, C. Kobryn and J. Given(1990): The Intelligent Monitoring System, Acdepted for publication in *Bull. Seism. Soc. Am.*.

Fyen, J. (1990): Diurnal and seasonal variations in the microseismic noise level observed at the NORESS array. *Phys. Earth Planet. Int.*, in press.

Kværna, T. (1989): On exploitation of small-aperture NORESS type arrays for enhanced P-wave detectability. *Bull. Seism. Soc. Am.*, 79 888–900.

Kværna, T. (1990): Sources of short-term fluctuations in the seismic noise level at NORESS. *Phys. Earth Planet. Int.*, in press.

Ringdal, F. (1976). Maximum-likelihood estimation of seismic magnitude. *Bull. Seism. Soc. Am.*, 66, 789–802.

Ringdal, F. and T. Kværna (1989): A multichannel processing approach to real time network detection, phase association, and threshold monitoring. *Bull. Seism. Soc. Am.*, 79, 1927–1940.

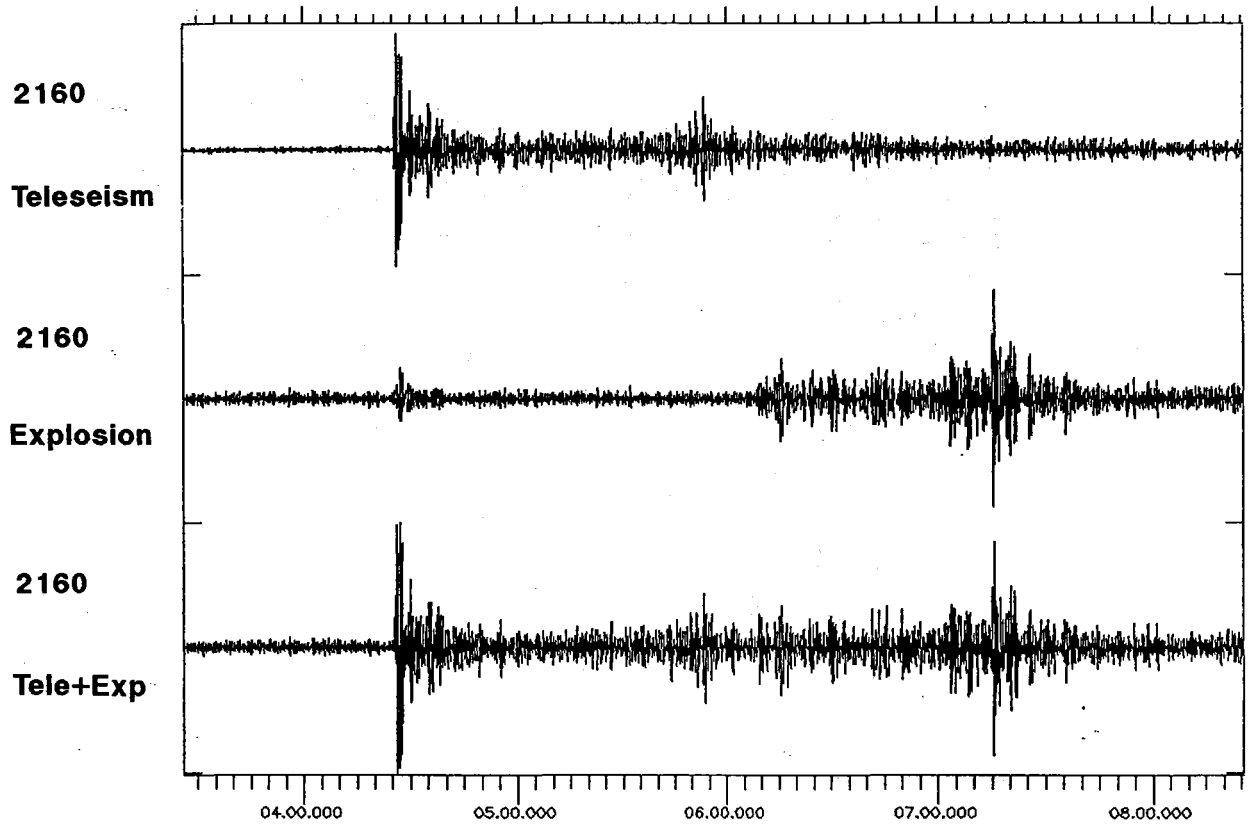

Fig. 7.6.1. Constructed example of a possible event interference, where a teleseismic P-phase is interfering with the Pn-phase of a regional event.

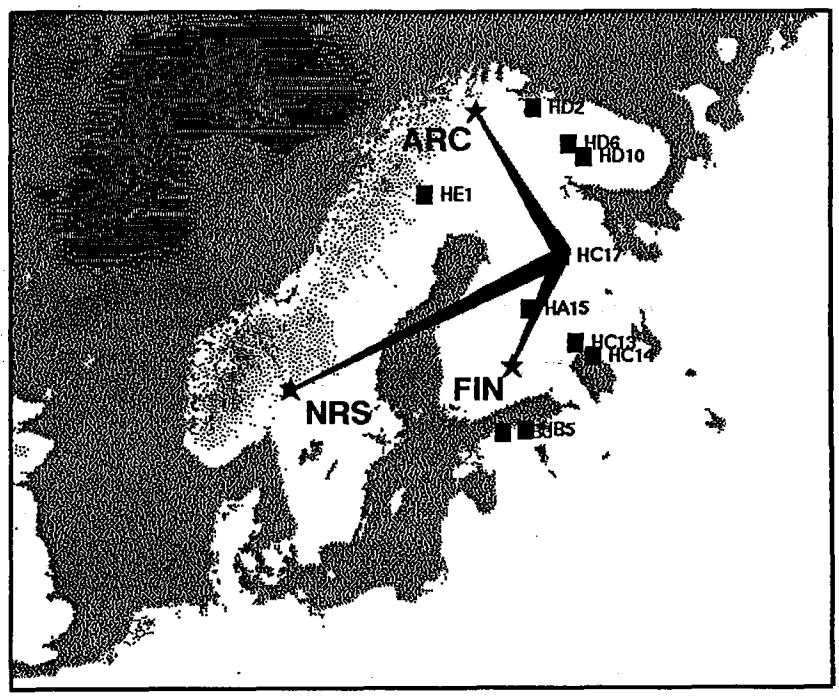

Fig. 7.6.2. The location of the mining regions subjected to threshold monitoring is shown by filled squares. The three regional arrays, NORESS, ARCESS and FINESA, are shown by stars. The filled sectors from each array to the mine HC17, serve to focus our interest to that particular mine location.

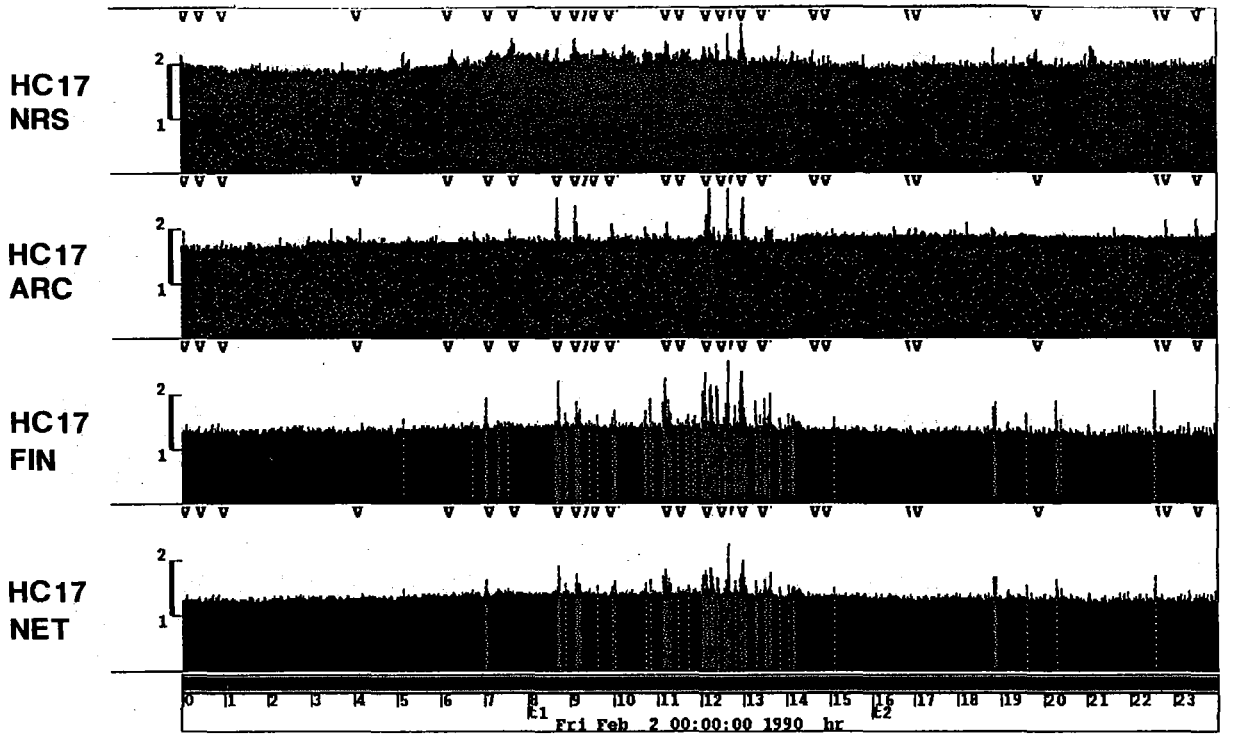

Fig. 7.6.3. The top three panels show the upper magnitude limits for mine HC17 for Friday 02/02/90, computed from the three regional arrays separately. The unit on the vertical axes is magnitude The lower panel shows the upper magnitude limit inferred from the network of arrays. The V's indicate origin times of events located by the IMS.

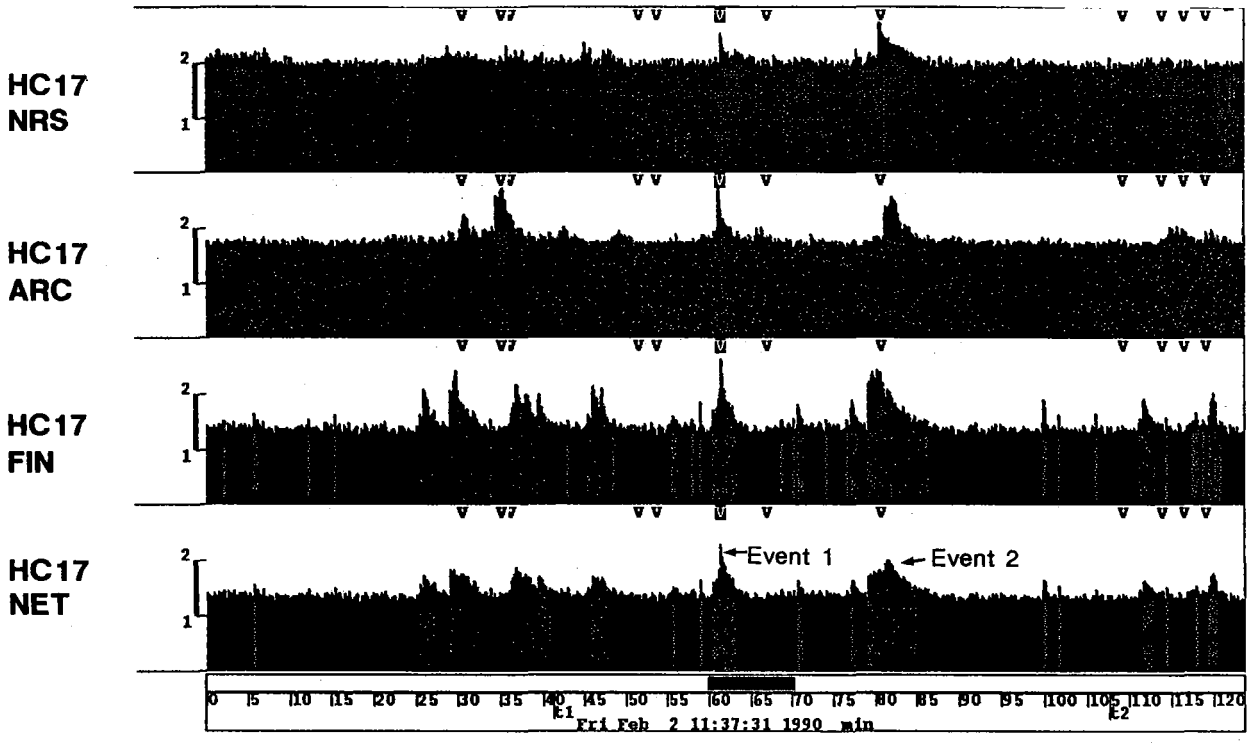

Fig. 7.6.4. This is a blowup of Fig. 7.6.3, with start time at 11.37.31. The length of the time interval is about 125 minutes. The two marked events are of special interest, since high upper magnitude limits are observed.

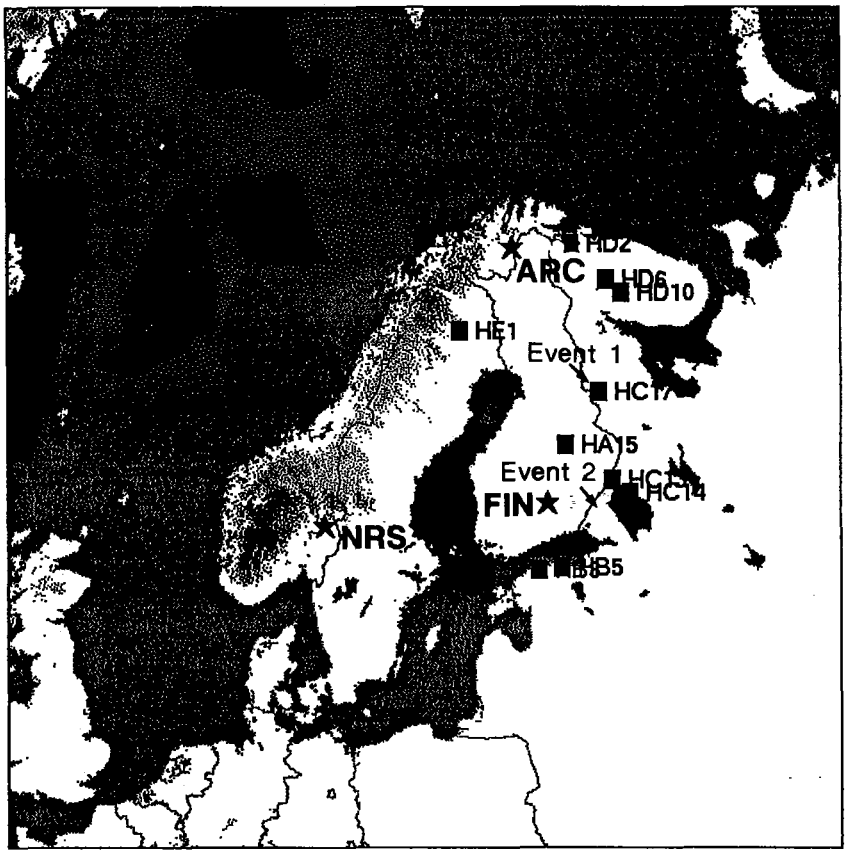

Fig. 7.6.5. Locations of the two events referred to in Fig. 7.6.4.

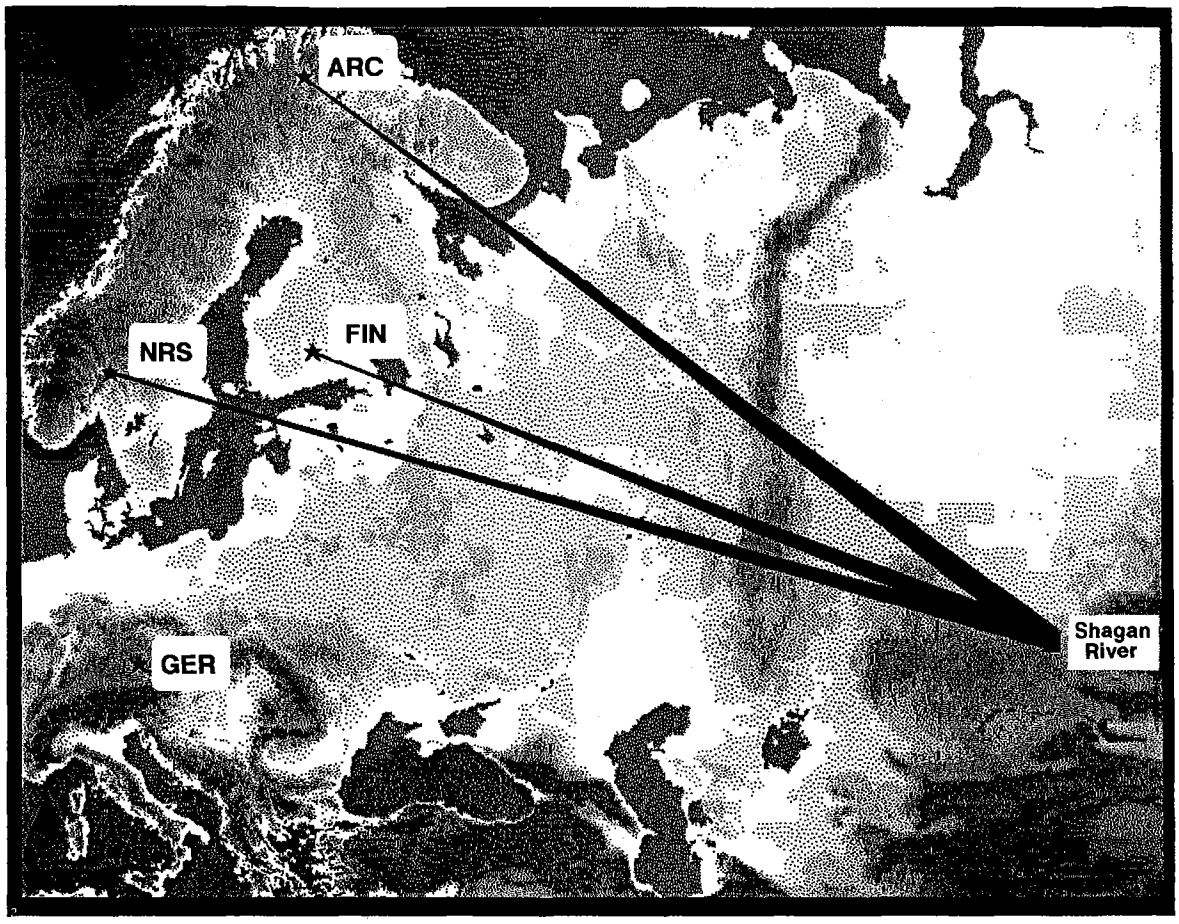

Fig. 7.6.6. This figure shows the location of the Shagan River test site, and also indicates the raypaths (approximated as straight lines) to NORESS, ARCESS and FINESA.